Synthesis of a Triazine-Based Hyper Branched Macromolecule Charring Agent and its Effect on Flame-Retardant Thermoplastic Polyester Elastomer to Improve Anti-Dripping

Zhengyi Wang
East China University of Science and Technology
Wei Wu (wuwei@ecust.edu.cn)
East China University of Science and Technology
Hongchen Lin
East China University of Science and Technology
Wenjing Zhang
East China University of Science and Technology
Xinzhu Xu
East China University of Science and Technology
Wei Wang
East China University of Science and Technology

Research Article

Keywords: Intumescent flame retardant, triazine charring agent, aluminum hypophosphite, flame retard TPEE composites.

Posted Date: April 20th, 2021

DOI: https://doi.org/10.21203/rs.3.rs-423227/v1

Abstract

A triazine-based charring agent (CDS) was synthesized and combined with diethyl aluminum hypophosphite (AlPi) to develop an intumescent flame retardant (IFR) system to improve thermoplastic polyester elastomer (TPEE) anti-dripping. The results showed that the limiting oxygen index (LOI) of the TPEE/15AlPi/5CDS composite reached 30.2%, and it passed the V-0 test in vertical combustion (UL-94). The results of thermogravimetric analysis (TGA) showed that CDS had good thermal stability and high char residue (50.8wt%) at 700°C. And when combined with AlPi added to TPEE, which can improve its char residue ranges from 1.68wt% to 23.52wt%. The structure evolution during the heating process was studied by heating infrared spectroscopy (IR), and the morphology and chemical structure of char residues were studied by scanning electron microscope (SEM) and laser Raman spectroscopy (LRS). The high-efficiency flame-retardant TPEE composite formed a continuous, dense and porous char layer containing triazine ring and aromatic ring structure after combustion.

1 Introduction

Thermoplastic polyester elastomer (TPEE) is a polymer that have the high elasticity of traditional vulcanized rubber at room temperature and can be plasticized and molded at high temperatures[1]. Because of its many advantages in use and processing performance, TPEE have been widely used in the electrical industry. However, limited by the molecular structure, TPEE are flammable, and are accompanied by melting and dripping during the combustion process, and cannot self-extinguish from the fire[2,3]. In recent years, with the continuous improvement of the requirements for material fire resistance and environmental protection performance, the research of flame retardant TPEE has become a hot spot[4-6].

Intumescent flame retardant (IFR) is a rapidly developing halogen-free flame retardant, usually composed of three components: acid source, gas source and carbon source and the flame-retardant mechanism is that the acid source catalyzes the dehydration of the carbon source into char[7]. The incombustible gas produced by the gas source expands the char layer and dilutes the concentration of combustibles in the combustion environment. Metal hypophosphite has been considered a friendly flame retardant and aluminum hypophosphite(AlPi) has proved to be effective in the fire resistant of polyester in recent year[8,9]. In our previous research in order to solve the problem of melt dripping in the combustion process of thermoplastic polyester elastomer, it was found that the intumescent flame retardant composed of aluminum hypophosphite and melamine phosphate can be used to improve the combustion performance of thermoplastic polyester elastomer[10-14]. However, the system still needs to add some synergists, such as novolac[10] montmorillonite[11] graphite[12], CNTs and MoS_2[13] to improve the charring performance of TPEE and achieve the purpose of preventing combustion. However, excessive addition of inorganic components will undoubtedly worsen the mechanical properties of TPEE. Therefore, it's of great significance for developing a new type of charring agent with high efficiency and stability.

Triazine flame retardants are triazine derivatives in molecular structure, and nitrogen flame retardants in flame retardant elements, which have the advantages of low toxicity, low smoke, recyclability, and environmental protection[15]. The flame retardant mechanism of triazine flame retardants is to release non-combustible gases such as N_2 and NH_3 during the flame retardant process to achieve gas phase flame retardancy. At the same time, the tertiary carbon structure of the triazine ring is aromatic, thermally decomposed to form a stable graphitized char layer, which realizes the condensed phase flame retardant during the flame retardant process. Junfeng Zhou[16], Caimin Feng[17,18] and others used cyanuric chloride and different organic diamines to copolymerize to form macromolecules with different triazines, which are compounded with acid sources to show excellent flame retardant properties in polymer materials, especially the ability to form char. And in our previous research, we found that the linear triazine charring agent can play a synergistic effect with diethyl aluminum hypophosphite, and can inhibit the droplet in the TPEE matrix to achieve the flame retardant effect[14].

In our follow-up research, we strive to synthesize a new type of hyper branched macromolecular charring agent in order to achieve a better cross-linking into charcoal effect to suppress the droplet of TPEE in the combustion process. In this work, a triazine-based bulk macromolecular charring agent (referred to as CDS in this article) was successfully synthesized. Flame-retardant TPEE composites were prepared using CDS and aluminum hypophosphinate as phosphorus flame retardants. Compared with the analogous triazine charring agents reported by other researchers, the incorporation of diamine as a chain extender makes the relative content of polar end-capping reagent in CFA higher, which can effectively moderate the compatibility between the charring agent and the hard molecular chains in TPEE, and improve the carbonization efficiency of CDS in the intumescent flame retardant TPEE systems. The further research was conducted on the mechanism of char forming process and the synergistic effect of CDS with AlPi on flame retardant process. The fire behavior, the thermal decomposition and the char formation mechanism of the flame retardant composites were studied by LOI test, UL-94 test, TGA, SEM and LRS.

2 Experimental Section

2.1 Materials

TPEE resin (H605, T_m=193℃, Shore Hardness=55D) was offered by Sunplas co., ltd(China). Cyanuric chloride (CNC, purity 99%) and Diethyl aluminum hypophosphite(AlPi) were purchased from Macklin Biochemical Co., Ltd. (Shanghai, China). 4,4-Diaminodiphenyl sulfone (DDS) was obtained from Lingfeng Chemical Reagent Co., Ltd. (Shanghai, China). Sodium carbonate ($NaCO_3$), 1,4-dioxane was supplied by Sinopharm Chemical Reagent Co., Ltd. (Shanghai, China).

2.2 Synthesis of CDS

As showed in Fig.1, the specific preparation route of CDS are as follows. 4,4-Diaminodiphenyl sulfone (0.09mol) and 400ml 1, 4-dioxane were added to a 1000ml four-necked flask with a thermometer and

mechanical stirring. And then the solution of cyanuric chloride (0.06mol) dissolved in 200 ml 1, 4-dioxane was drop-wise added into the flask in 2 h at 25℃. After all the ingredients were added in the reaction system, the reacting mixture was stirred at 95℃for 10 h. The by-products Cl generated during the reaction are neutralized by the reaction with Na_2CO_3. Finally, the reaction mixture was filtered and washed several times to remove the solvent, NaCl, $NaHCO_3$ and the excessive Na_2CO_3.After drying in a vacuum oven at 120℃ for 4 h, light yellow product was obtained and the yield is 92.2%.

2.3 Preparation of flame retardant TPEE samples

TPEE, AlPi, CDS were dried in a 90℃ constant temperature drying oven (DHG-9055A, Shanghai Hecheng Instrument Manufacturing Co., Ltd.) for 8 hours, and weighed according to the research formula. All the components were melt-mixed in a torque rheometer (160 Nm/Polab QC, Germany Haake Company) at 205℃and 60 r/min rotor speed. Specifically, the premix of TPEE and CDS was firstly added into torque rheometer and mixed for 3.5 min, and then AlPi were added and melt-mixed for another 2.5 min. After that, all the components were press molding on a flat vulcanizer (QLB-50, Shanghai Rubber Machinery First Factory) at 205℃. After hot-pressed for 5 min and holding pressure for 4 min, all samples were cold-pressed to room temperature to obtain suitable test specimens.

2.4 Characterization

The Fourier transform infrared was obtained with a Nicolet FTIR 6700 infrared spectrophotometer where the samples were prepared with KBr pellets.

The ^{13}C solid-state NMR spectra were measured on a Thermo Varian INOVA500NB spectrometer at 500 MHz.

The vertical burning test (UL-94) was performed with a CFZ-3 type instrument (Jiangning Analysis Instrument Company, China) according to ASTM D3801-10 standard with specimen size of 130.0 mm × 13. 0mm × 1.6 mm.

The Limiting oxygen index (LOI) was performed by an oxygen index instrument (JF-3, Jiangning Analysis Instrument Factory, China) with specimen size of 130.0 mm× 6.0 mm × 3.0 mm according to ASTM D2863-17.

The thermogravimetric analysis (TGA) was performed using a STA 409 PC/PG thermogravimetric analyzer (Netzsch, Germany) at a heating rate of 10 ℃/min, heating from room temperature to 700 ℃ under air atmosphere (40 mL/min).

The microstructure of char residues was examined with field emission scanning electron microcopy (SEM S-3400, Japan) with accelerating voltage was 15.0 KV. The sample were sputter-coated with a conductive layer of gold before analysis.

The graphitic degree of char residues was characterized by Laser Raman spectroscopy (SPEX, USA) with a 532 nm argon laser line at room temperature, the scanning range was 400 ~ 2000 cm^{-1} region.

3 Results And Discussion

3.1 Characterization of CDS

The structural characterization of CDS was performed by FTIR and ^{13}C-NMR. The FTIR spectra of DDS, CDS and CNC were presented in Fig.2. Clearly, several functional groups from DDS and CNC, such as N-H(3320-3530cm^{-1}), C=C (1620-1450cm^{-1}), C=N(1530cm^{-1}), can be observed in the FTIR spectra of CDS. The absorption peak of C-N(1265cm^{-1}) appeared, and the absorption peak of C-Cl(850cm^{-1}) disappeared, which indicated the completion of polymerization. The structures of CDS was further confirmed by ^{13}C solid-state NMR in Fig.3. The signals at 165.75 ppm, 142.49 ppm, 136.08ppm, 128.85 ppm, 121.30 ppm were attributed to C (a, δ_{tr-C}), C (b, $\delta_{C=C}$-in *para*-point of benzene ring), C (e, $\delta_{C=C}$-in *para*-point of benzene ring), C (d, $\delta_{C=C}$-in *meta*-point of benzene ring), C (c, $\delta_{C=C}$-in *ortho*-point of benzene ring), respectively.

3.2 Flame retardancy of TPEE composites

The formula and the results of LOI values and UL-94 ratings of neat TPEE and TPEE composites are shown in Table1 and Table 2. Neat TPEE was very flammable and burned to the clamp after the first ignition, and was accompanied by severe droplets with the LOI value of 17.9. CDS was acted as both charring and blowing agents in the intumescent flame retardant system. There was hardly any improvement for the LOI values and UL-94 ratings by the addition of 20% CDS separately. It revealed that the lack of acid source for the intumescent flame retardant system is not efficient enough. When 15wt% or 20wt% of AlPi was added, the TPEE sample were extinguished in about 5 seconds after the Bunsen burner is ignited for 10 seconds, and then during the secondary combustion, droplets dripped into the fire Bunsen burner constantly. Therefore, it reaches the Ul-94 V-2 grade. In addition, compared with neat TPEE, the LOI values of TPEE/15AlPi and TPEE/20AlPi increased to 26.8 and 24.5, which showed that aluminum hypophosphite was able to play a flame retardant effect in both condensed phase and gas phase. In the gas phase, free radical capture leaded to flame suppression, and in the condensed phase, it initiated the formation of char or inorganic residues[19].

The formulation of TPEE composites and results of LOI and UL94 test of all the investigated samples were shown in Table 1 and Table 2 respectively. As the mass ratio of the acid source and the char source increased, it can be seen that when 2 wt% CDS was added into the intumescent flame retardant system, the LOI of the TPEE/18AlPi/2CDS was increased to 28.2. However, droplets were still produced during the secondary combustion and V-2 rating was reached, which meant less char agent was unable to form a thick and dense char layer to prevent melt dripping. With the increase in the proportion of CDS,

TPEE/15AlPi/5CDS can stop burning during the first combustion in 2.2 seconds and the UL-94 rating was enhanced to V-0 from V-2 with inhibited dripping during the secondary combustion. However, with the further increase of the charring agent, it can be found that the LOI value of TPEE/10AlPi/10CDS was decreased to 26.2 and dripped again within 10s in the ignition process of secondary flame. The reason was that the char layer formed after expansion and combustion was too much to cover the surrounding of the sample, making the heating area larger. It can be concluded that an appropriate ratio of AlPi and CDS in the intumescent flame retardant system was particularly important for the flame retardant performance of TPEE composites.

Table 1 Composition of formulas (wt%)

Sample	TPEE	AlPi	CDS
Neat TPEE	100	0	0
TPEE/20AlPi	80	20	0
TPEE/20CDS	80	0	20
TPEE/18AlPi/2CDS	80	18	2
TPEE/15AlPi/5CDS	80	15	5
TPEE/10AlPi/10CDS	80	10	10
TPEE/15AlPi	85	15	0

Table 2 Results of LOI and UL94 test of all the investigated samples

Sample	LOI(%)	UL-94,1.6mm Bar		
		t_1/t_2	Dripping	Rating
Neat TPEE	17.9±0.5	BC	Yes/-	NR
TPEE/15AlPi	26.5±0.5	6.2/14.2	No/Yes[a]	V-2
TPEE/20AlPi	29.8±0.5	4.5/10.5	No/Yes	V-2
TPEE/20CDS	22.5±0.5	BC	Yes/-	NR
TPEE/18AlPi/2CDS	28.2±0.5	4.5/8.9	No/Yes	V-2
TPEE/15AlPi/5CDS	30.2±0.5	2.2/5.9	No/No	V-0
TPEE/10AlPi/10CDS	26.2±0.5	4.5/8.9	No/Yes	V-2

LOI: limiting oxygen index; t_1: average combustion time after the first application of flame; t_2, average combustion time after the second application of flame; BC: burns to clamp; NR: no rating.

[b] No/yes corresponds to the first/second flame application.

3.3 Charring behavior and thermal degradation of CFA and AlPi

Table 3 Results of thermogravimetric analysis under N_2 atmosphere

Sample	$T_{5\%}$	$T_{10\%}$	T_{max}	dw/dt□max□	Residue(%)
	(℃)	(℃)	(℃)	□wt%/min^{-1}□	700(℃)
CDS	336.1	361.3	403.2	-0.30	50.8
AlPi	436.6	451.4	482.8	-2.28	20.98
IFR	394.3	423.8	391.0	-1.22	32.24
Calculation IFR	409.2	445.6	396.0	-1.31	28.44

In order to investigate the charring behavior and thermal degradation of CDS, AlPi and IFR during heating, thermal gravimetric analysis was used. IFR was AlPi/CDS mixture whose mass fraction was 15:5 and calculation IFR was the result calculated from the experimental results of AlPi and CDS based on their percentage in the IFR system in accordance with formula (1).

$$W_{calculation\ IFR}=W_{AlPi}*15/20+W_{CDS}*5/20 \quad (1)$$

As can be seen from table.3, AlPi showed excellent thermal stability with a high char residue (20.98%) at 700℃ under N_2 atmosphere. And it decomposed into one steps, starting from 436.6℃ and the maximum mass rate at 482.8℃. AlPi can catalyze dehydration and cross-linking reaction of charring agents in IFR, and serves as an acid source and CDS can be used as a charring and forming agent. The thermal degradation process of CDS was divided into two steps: the first step roughly occurs at 300 to 400°C (corresponding to the chemical reaction of dehydration and release of SO_2)[20], and the second step occurred at 400 to 550°C, which may be allocated to the decomposition of macromolecular framework. And finally, CDS degraded into expanded char during the pyrolysis process with the increase of temperature, and the char residue is about 50.8% at 700°C. These results showed that CDS had good thermal degradability, which can be attributed to the presence of triazine and benzene ring.

The initial decomposition temperature ($T_{5\%}$) of IFR was 394.3℃ and the char residue was 32.24% at 700℃, which proved that IFR had excellent thermal stability and charring performance. Compared with Calculation IFR, the calculated value of initial decomposition temperature was 409.2 ℃, which was higher than the actual measured temperature value. This result revealed that with the incorporation of CFA into AlPi, the overall thermal degradation process changed. Meanwhile, the char residue (28.44%) of calculation IFR was lower than the IFR, which indicated that AlPi can improved the charring performance of CDS and accelerated the formation of the char layer.

3.4 Thermal degradation of TPEE and TPEE composites

Figure 6 and Figure 7 showed the TGA and DTG curves of TPEE and flame-retardant TPEE composites under N_2 atmosphere. Table 4 summarized detailed data such as 5% mass loss, 10% mass loss, maximum mass loss rate, and the experimental and calculation value of char residue at 700°C. Through these data, we tried to explore the mechanism of the condensed phase and clarify the thermal stability of different formulations. The decomposition of neat TPEE started at 370.2℃, and the highest loss rate at 403.2℃ was -2.53 wt%/min^{-1}. After the TGA test, TPEE was completely degraded into gaseous molecules, so it can be decomposed in one step with almost no residue. After AlPi was added to the TPEE matrix, the initial thermal decomposition temperature ($T_{5\%}$) and the maximum thermal decomposition rate temperature(T_{max}) of the TPEE composite did not change much, which indicated that AlPi can cooperate with the TPEE matrix well, and the experimental value of char residue of the composite was much higher than the calculated value, which indicated that the phosphorus in AlPi can catalyze TPEE to form a char layer during the combustion process. When the intumescent flame retardant composed of CDS and AlPi was added to TPEE, the initial thermal decomposition temperature of the composite material is slightly reduced, which was due to the lower initial thermal decomposition temperature of CDS. The proportion increased gradually, and it was found that when the addition amount of the charring agent CDS was 5%, the synergistic efficiency of AlPi and CDS was the highest at this time, and the char residue of the TPEE composite material was increased to 23%, which meant the surface can form a thick and dense char layer to prevent the TPEE composite from dripping so that the flame retardancy would be improved, which was consistent with the UL-94 measurement result. Comparing all formulas from TPEE/18AlPi/2CDS to TPEE/10AlPi/10CDS, the experimental values of the char residue rate were always much higher than the calculated values, which showed that the role of the intumescent flame retardant was not a simple linear addition, but was caused by the good synergy between the acid source, the charring agent and the matrix.

Table 4. Results of thermogravimetric analysis under N_2 atmosphere.

Sample	$T_{5\%}$	T_{max}	dw/dt（max）	Residue(700°C, N_2)	
	(°C)	(°C)	（wt%/min^{-1}）	Cal	Exp
Neat TPEE	370.3	403.2	-2.53	-	1.68
TPEE/20AlPi	368.3	397.0	-2.17	5.54	16.50
TPEE/18AlPi/2CDS	360.5	402.1	-1.71	6.14	19.12
TPEE/15AlPi/5CDS	352.0	391.0	-1.82	7.03	23.52
TPEE/10AlPi/10CDS	341.4	396.0	-1.50	8.52	17.72
TPEE/15AlPi	368.7	396.0	-2.14	4.58	16.08

$T_{5\%}$: temperature of 5 wt% mass loss; T_{max}: temperature of the maximum mass loss rate; dw/dt(max): maximum mass loss rate; Residue: weight of the residue at 700°C after thermogravimetric analysis test; Cal: calculation value of char residue; Exp: experimental Value of char residue.

3.5 Dynamic FTIR of TPEE and TPEE composites

Through the characterization of the infrared spectrum of the TPEE composites during the heating process, the synergistic effect between flame retardants and the mechanism and form of action in the matrix can be studied. Figure.8-10 showed the infrared spectra of Neat TPEE, TPEE/AlPi and TPEE/AlPi/CDS at a heating rate of 10°C/min^{-1}. 2962cm^{-1} and 2878cm^{-1} (-CH_2, stretching vibration), 1712cm^{-1} (-C=O, stretching vibration), 1458cm^{-1} (-CH_2, fracture vibration), 1410cm^{-1} (aromatic) ring), 1274cm^{-1} (-CO-O-ester), 1106cm^{-1} (-CH_2-O-CH_2-ether) and 727cm-1 (-CH, bending vibration of aromatic ring) were the characteristic peaks of TPEE. With the increase of heating temperature, the band intensity at 2956 and 2861 cm^{-1} (-CH_2) dropped rapidly, which was caused by the scission of the α-methylene group in the soft segment, which was consistent with our previous research results[21].

For the formula TPEE/15AlPi, due to the addition of AlPi, the typical absorption bands of AlPi appeared in the spectrum, such as 1151, 1079 and 780 cm-1 (-P = O); 1018 cm-1 (PO_4^{3-}); and 475cm-1 (O=PO, AlPi). Same as Neat TPEE, TPEE/15AlPi in Fig.9 was also decomposed on the soft segment due to the active a-methylene group of the ether bond. In the hard segment (C=O), due to the presence of carboxyl groups, there was a shoulder gap at 1680cm^{-1}. As the temperature rose, due to the strong interaction between Al^{3+} and carboxyl groups, electron migration occurred, which also improved the thermal stability of the composite. There was no P-O-H unit (3400-3800cm^{-1}) from the curve at 450°C, which indicated that the diethyl aluminum hypophosphite may played a flame retardant effect in the gas phase after being released. The solid phase spectrum of TPEE/AlPi showed that the interaction between TPEE and AlPi improved thermal stability and increased the residue rate, and may formed intermediate products in the gas phase to suppress flames.

The infrared spectrum of TPEE/15AlPi/5CDS during the heating process was shown in Figure.10. It can be seen that the N-H peak at 3400cm^{-1} gradually weakened with the increase of temperature, which indicated that the triazine charring agent CDS decomposed non-combustible gases such as ammonia and nitrogen, thereby exerting a flame retardant effect in the gas phase. In addition, C-N (1265cm^{-1}), C=N (1500cm^{-1}) and characteristic bands of aromatic structure 737cm^{-1} and 1411cm^{-1} appeared in the residue at 450℃, which indicated that the addition of triazine charring agent CDS can make the TPEE composites form the char layer spliced by benzene ring and triazine ring after combustion, thereby increasing the strength of char.

3.6. Morphology and chemical structure of char residues

Raman spectroscopy was widely used to study the crystal structure and molecular structure of carbon materials. In addition to analyzing the morphology of char residue at high temperature, the study of the structure of char residue was of great significance to the research of the flame retardant mechanism. Figure.11 showed the Raman spectra of TPEE / 20AlPi, TPEE / 18AlPi / 2CDS and TPEE / 15AlPi / 5CDS after calcination in a muffle furnace at 700°C for 15 minutes and it can be found that there were broad peaks of 1332 cm^{-1} and 1590 cm^{-1} in the Raman spectrum The former (D-band) was caused by the vibration of the disordered graphite sp^3 hybrid atom or the swinging carbon atom on the amorphous char layer, and the latter (G-band) corresponds to the vibration of the sp^2 hybrid atom of the graphite sheet. The degree of graphitization of the system can be expressed by the ratio of the peak areas of the D band and the G band (I_D/I_G). Generally speaking, the lower the I_D/I_G, the more graphitic carbon in the char layer, and the higher the quality of the char layer. The higher the degree of graphitization, the denser and stable the structure of the carbon layer. It can be seen from Figure 11 that the I_D/I_G ratio of TPEE/20AlPi (2.645) was higher than that of TPEE/18AlPi/2CDS (2.226), which indicated a decrease in the degree of graphitization in the residual carbon. However, compared to TPEE/18AlPi/2CDS, the I_D/I_G ratio of TPEE/15AlPi/5CDS (1.835) reduced, which suggested that the mass percentage of graphitized carbon in carbon was increased. The graphitized carbon formed in the combustion process was of great significance for controlling the release of heat and volatiles from the stable carbon structure at high temperatures. The I_D/I_G ratio followed the order of TPEE/20ALPi <TPEE/18AlPi/2CDS<TPEE/15AlPi/5CDS, which showed that TPEE/15AlPi/5CDS had the highest degree of graphitization and the best thermal stability. And this was also in line with the improvement in flame retardancy mentioned above.

Figure.12 showed the SEM image of the residual carbon after calcination in a muffle furnace at 700°C for 15 minutes. It can be seen from the figure that the char residue of the TPEE/15AlPi had many obvious defects, and the surface was irregular. Such a structure cannot effectively prevent the heat transfer from being transferred to the substrate, nor can it prevent the molten combustion material from dripping. As for Figure.12(b), due to the addition of a small amount of the charring agent CDS, the carbonization of CDS accelerated the carbonization speed of the composites, thereby forming a thick carbon layer, which can

slow down the heat transfer. However, due to the lack of carbon source, it was not enough to form a dense enough char layer to prevent dripping. Further adding CDS, it can be seen from Figure.12(c) that the residue of the TPEE/15AlPi composite was dense, porous, and folded structure char layers, which can deposit char residues on the surface while blocking heat insulation. In addition, CDS can be used as a gas source after combustion, and non-combustible gases such as N_2, NH_2 and CO_2 were generated, which played the role of inflation, thereby diluting the concentration of oxygen on the surface of the composites and reducing the back diffusion of oxygen. These reasons had also prompted the composites to pass the V-0 UL-94 test. The above results showed that the intumescent flame retardant 15CDS/5AlPi had a good flame retardant effect and can play a role in the condensed phase and the gas phase.

3.7. Proposed flame-retardant mechanism

According to the described structure characterization and char formation behavior analysis, the possible flame retardant mechanism of TPEE / 15AlPi / 5CDS composite was shown in Fig.13 and Fig.14. Firstly, the charring agent CDS decomposed at about 336°C to release incombustible gas, and then cracks to generate triazine ring structures and aromatic structures, which were easy to assemble and splice into a char layer. Subsequently, the thermal oxidative degradation of the TPEE matrix occurred selectively in the soft segment of the polyether, and at the same time, the ester bond was formed. When the temperature continued to be oxidized, the polyester segment will also be broken. The chain scission reaction passes through a six-membered ring intermediate product, -COO abstracted the H atom from the methylene group at the β position to form an oligomer with a carboxyl group and an unsaturated double bond at the end, which continued to oxidize to produce tetrahydrofuran, butadiene, benzoic acid, water, CO2, etc.[22]. Subsequently, the Al^{3+} provided by AlPi after the temperature raised and the carboxyl-containing oligomers produced by the degradation of TPEE formed a compound, and finally a variety of inorganic aluminum phosphate salts such as pyrophosphate were formed. This phosphate had a certain strength and can help to isolate hot oxygen exchange. In addition, the phosphate closely covered the surface of the substrate to further catalyze the carbonization of the TPEE substrate and the triazine charring agent CDS. Finally, the decomposition of CDS produced an aromatic structure that was assembled with the pyrolysis product of TPEE, and the graphitized char layer was formed on the surface of the composites to isolate heat and play a flame retardant effect.

4 Conclusions

In this paper, a new type of charring agent CDS was synthesized by CNC, DDS through condensation reaction, which can form an IFR system together with AlPi, and the IFR significantly improved the flame retardancy of TPEE. When only 20% IFR was loaded, the TPEE composite can obtain a high LOI value of 30.2% and passed UL-94 V-0 rating. Through the analysis of TGA, it can be seen that CDS has an extremely high char residue rate and had a certain synergistic flame retardant effect with AlPi. Combining the structure analysis of heating infrared and the analysis of SEM and LRS charring behavior, it can be

concluded that CDS was an agent with excellent thermal stability and charring performance. It can be flame retardant when combined with AlPi to form intumescent flame retardant TPEE materials, and can form a high-quality graphitized carbon layer on the surface of the substrate.

References

1. Fang W, Fan X D, Jiao H Q, et al. Characterization and Properties of Thermoplastic Polyether Elastomer/Polyoxymethylene Blends Prepared by Melt-Mixing Method[J]. Polymer Science Series A, 2019, 61(6): 890-896.
2. Huang J, Wang J, Qiu Y, et al. Mechanical properties of thermoplastic polyester elastomer controlled by blending with poly(butylene terephthalate)[J]. Polymer Testing, 2016, 55: 152-159.
3. Wang W, Lu W, Goodwin A, et al. Recent advances in thermoplastic elastomers from living polymerizations: Macromolecular architectures and supramolecular chemistry[J]. Progress in Polymer Science, 2019, 95: 1-31.
4. Zhou Y F, Li W G, Chen C F, et al. An FT-IR study of the effect of added flame retardant on the structure of TPEE[M]. 2007: 590-592.
5. Kim S, Linh P T T, Kang J, et al. Phosphorus-containing thermoplastic poly(ether ester) elastomers showing intrinsic flame retardancy[J]. Journal of Applied Polymer Science, 2017, 134(46).
6. Zou L Y, Zhou M, Liu J Y, et al. Flame-retardant thermoplastic polyester based on multiarm aluminum phosphinate for improving anti-dripping[J]. Thermochimica Acta, 2018, 664: 118-127.
7. Bourbigot S, Duquesne S. Fire retardant polymers: recent developments and opportunities[J]. Journal of Materials Chemistry, 2007, 17(22): 2283-2300.
8. Li S, Yan H, Feng S, et al. Phosphorus-containing flame-retardant bismaleimide resin with high mechanical properties[J]. Polymer Bulletin, 2016, 73(12): 3547-3557.
9. Lu S Y, Hamerton I. Recent developments in the chemistry of halogen-free flame retardant polymers[J]. Progress in Polymer Science, 2002, 27(8): 1661-1712.
10. Zhong Y, Wu W, Wu R, et al. The flame retarding mechanism of the novolac as char agent with the fire retardant containing phosphorous–nitrogen in thermoplastic poly(ether ester) elastomer system[J]. Polymer Degradation and Stability, 2014, 105: 166-177.
11. Zhong Y, Jiang C, Ruan M, et al. Preparation, thermal, and flammability of halogen-free flame retarding thermoplastic poly(ether-ester) elastomer/montmorillonite nanocomposites[J]. Polymer Composites, 2016, 37(3): 700-708.
12. Zhang L, Wang L, Fischer A, et al. Effect of graphite on the flame retardancy and thermal conductivity of P-N flame retarding PA6[J]. Journal of Applied Polymer Science, 2018, 135(31).
13. Zhong Y, Li M, Zhang L, et al. Adding the combination of CNTs and MoS2 into halogen-free flame retarding TPEE with enhanced the anti-dripping behavior and char forming properties[J]. Thermochimica Acta, 2015, 613: 87-93.

14. Liu C, Zhang L, Mu L, et al. Synergistic effects between a triazine-based charring agent and aluminum phosphinate on the intumescent flame retardance of thermoplastic polyether ester[J]. Journal of Macromolecular Science, Part A, 2019, 56(7): 723-732.
15. Mishra N, Vasava D. Recent developments in s-triazine holding phosphorus and nitrogen flame-retardant materials[J]. Journal of Fire Sciences, 2020, 38(6): 552-573.
16. Zhou J, Wang J, Jin K, et al. s-Triazine-based functional monomers with thermocrosslinkable propargyl units: Synthesis and conversion to the heat-resistant polymers[J]. Polymer, 2016, 102: 301-307.
17. Feng C, Liang M, Jiang J, et al. Synergistic effect of ammonium polyphosphate and triazine-based charring agent on the flame retardancy and combustion behavior of ethylene-vinyl acetate copolymer[J]. Journal of Analytical and Applied Pyrolysis, 2016, 119: 259-269.
18. Feng C, Li Z, Liang M, et al. Preparation and characterization of a novel oligomeric charring agent and its application in halogen-free flame retardant polypropylene[J]. Journal of Analytical and Applied Pyrolysis, 2015, 111: 238-246.
19. Tang G, Wang X, Xing W, et al. Thermal Degradation and Flame Retardance of Biobased Polylactide Composites Based on Aluminum Hypophosphite[J]. Industrial & Engineering Chemistry Research, 2012, 51(37): 12009-12016.
20. Tang W, Qian L, Chen Y, et al. Intumescent flame retardant behavior of charring agents with different aggregation of piperazine/triazine groups in polypropylene[J]. Polymer Degradation and Stability, 2019, 169.
21. Zhong Y, Wu W, Lin X, et al. Flame-retarding mechanism of organically modified montmorillonite and phosphorous-Nitrogen flame retardants for the preparation of a halogen-free, flame-retarding thermoplastic poly(ester ether) elastomer[J]. Journal of Applied Polymer Science, 2014, 131(22): n/a-n/a.
22. Mi H Y, Jing X, Napiwocki B N, et al. Biocompatible, degradable thermoplastic polyurethane based on polycaprolactone-block-polytetrahydrofuran-block-polycaprolactone copolymers for soft tissue engineering[J]. Journal of Materials Chemistry B, 2017, 5(22): 4137-4151.

Figures

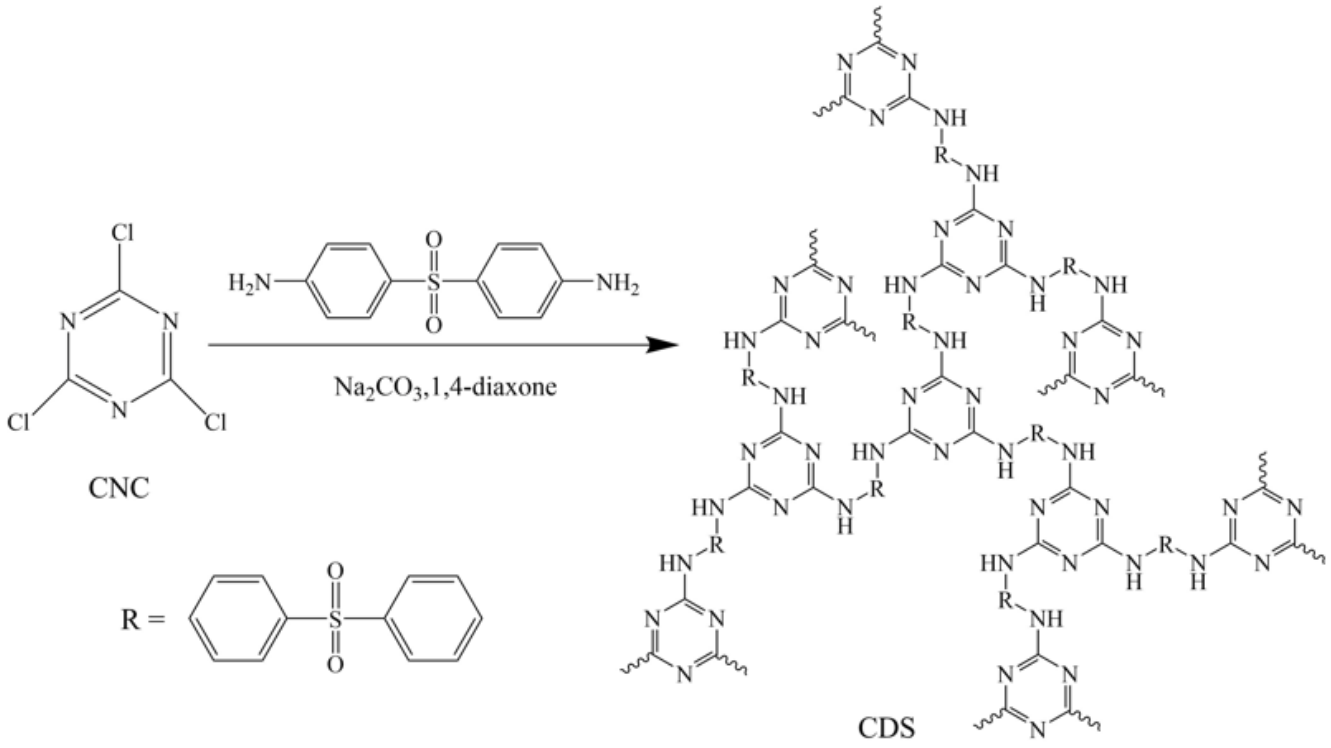

Figure 1

Synthesis of CDS

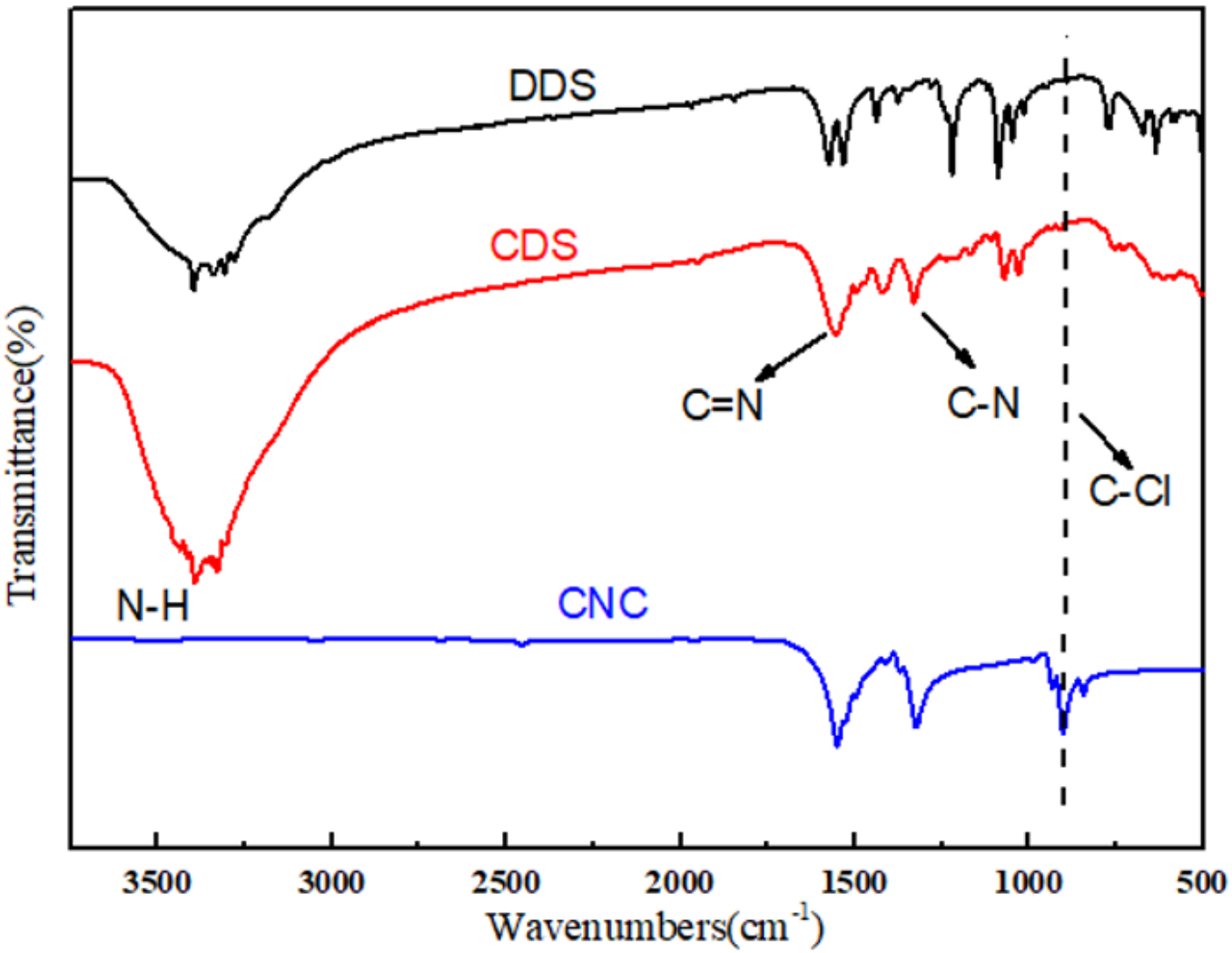

Figure 2

FTIR spectrum of DDS, CDS and CNC.

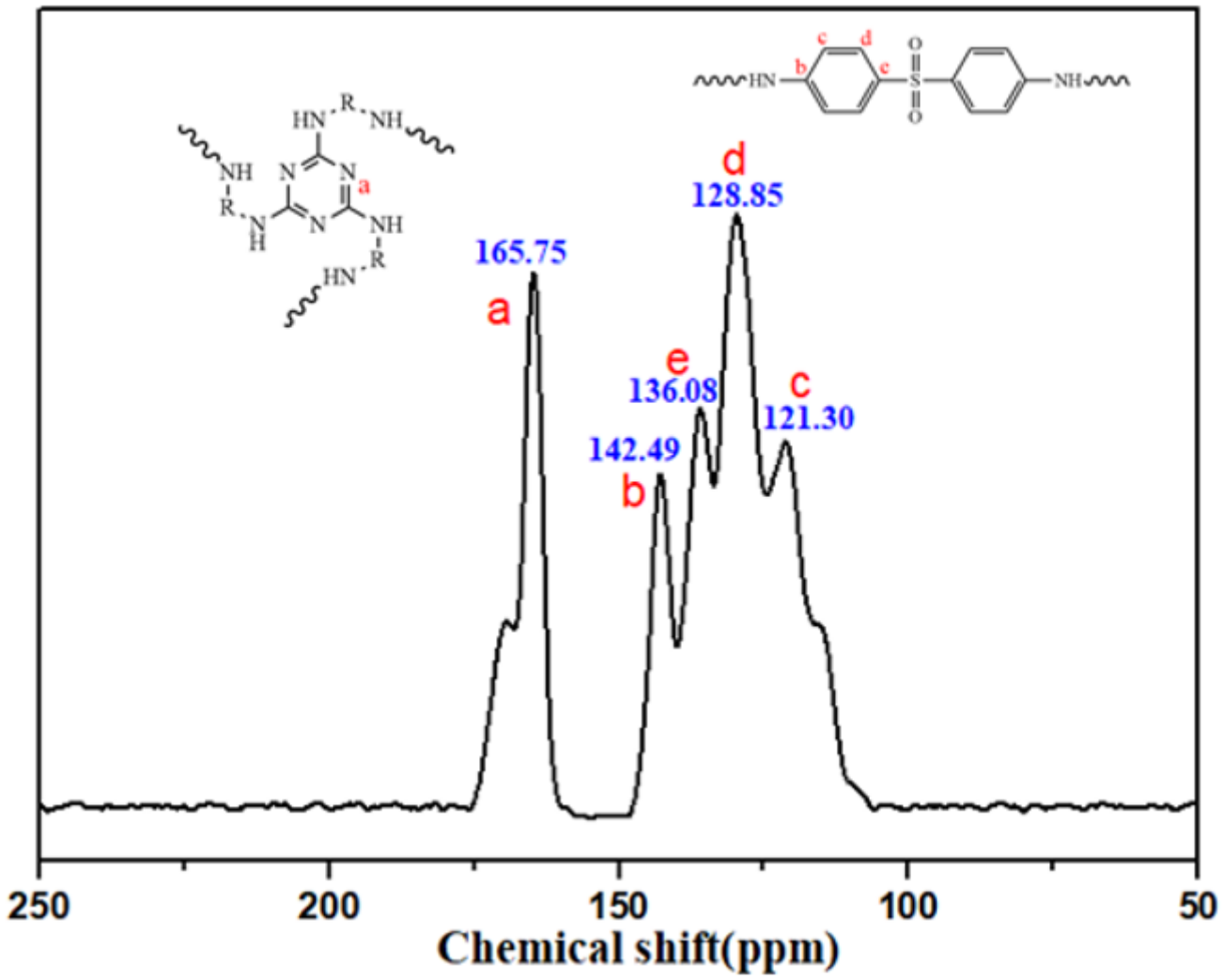

Figure 3

13C solid-state NMR spectrum of CDS.

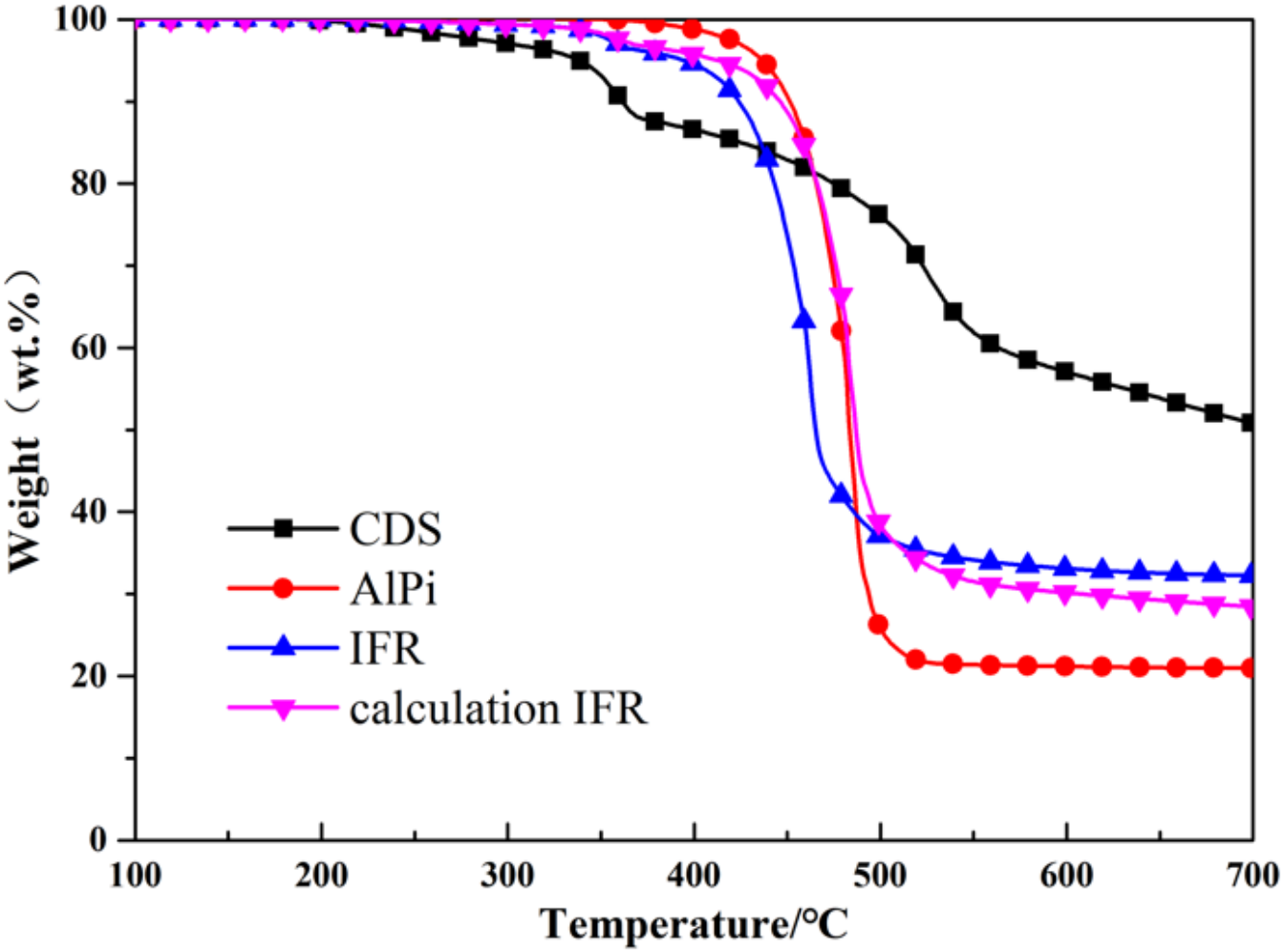

Figure 4

Mass loss curves of CDS, AlPi, IFR and calculation IFR (under nitrogen atmosphere, heating rate of 10°C/ min-1).

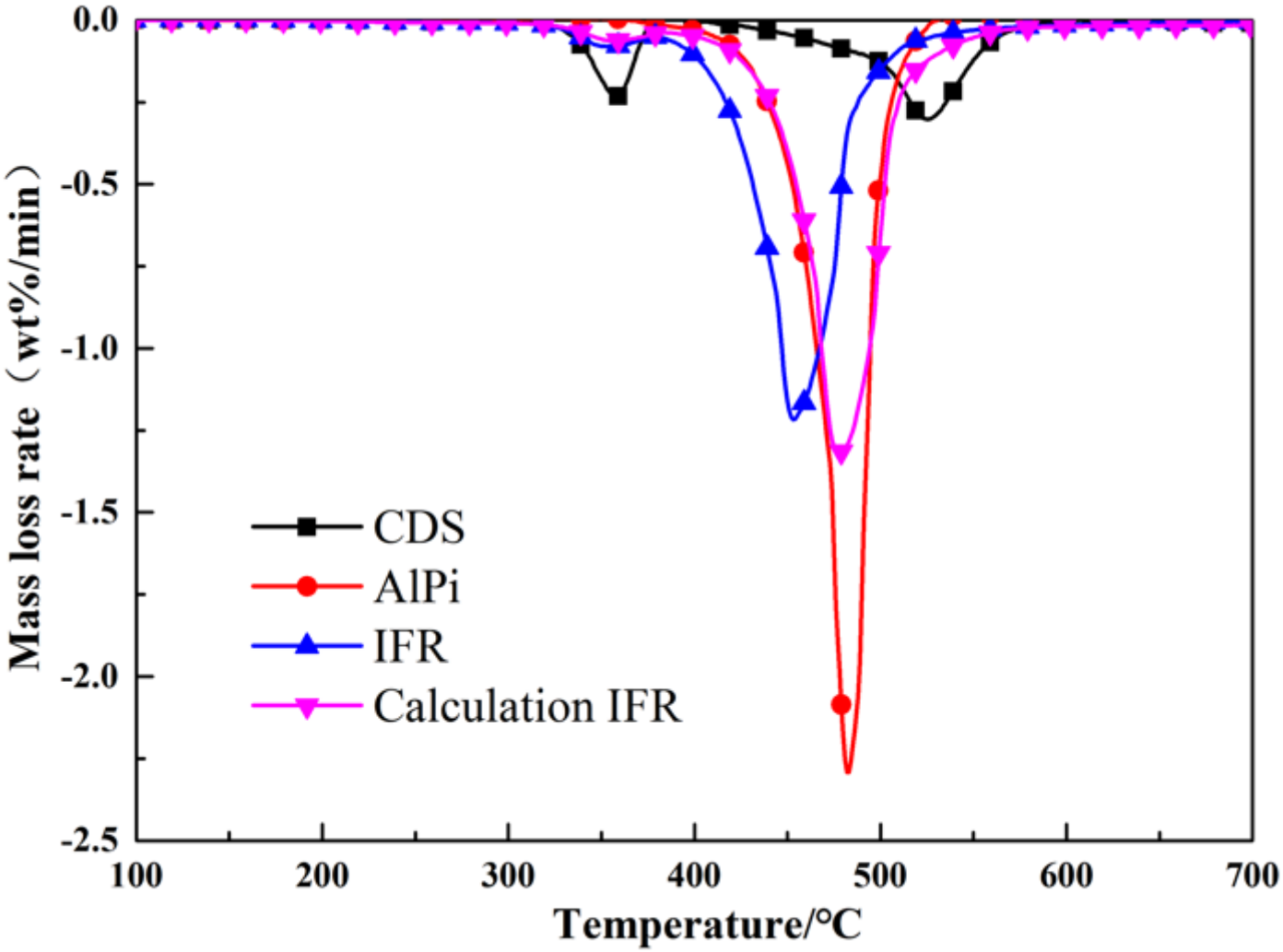

Figure 5

Mass loss rate curves of CDS, AlPi, IFR and calculation IFR (under nitrogen atmosphere, heating rate of 10℃/ min-1)

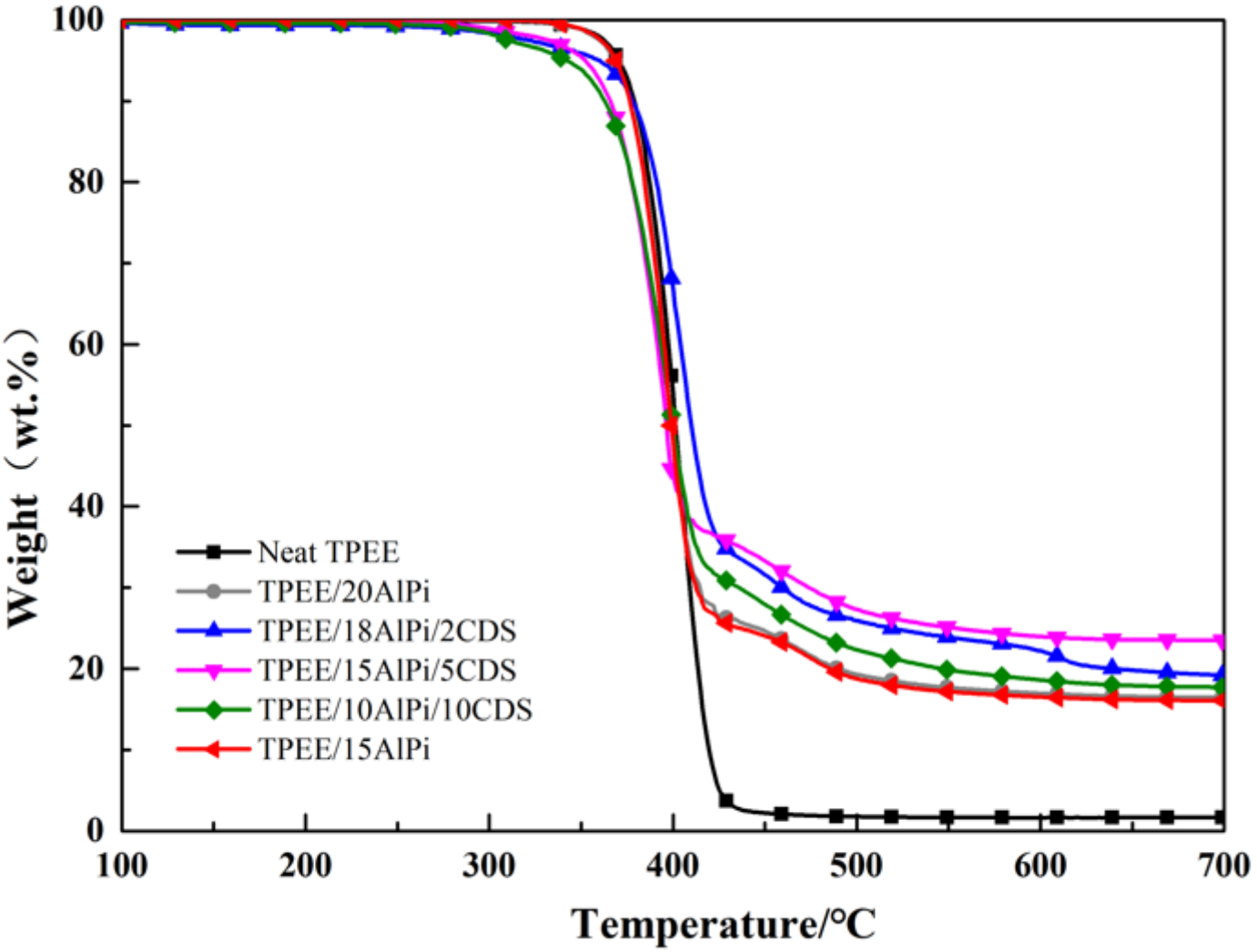

Figure 6

Mass loss curves of all the investigated samples (under nitrogen atmosphere, heating rate of 10°C/ min-1).

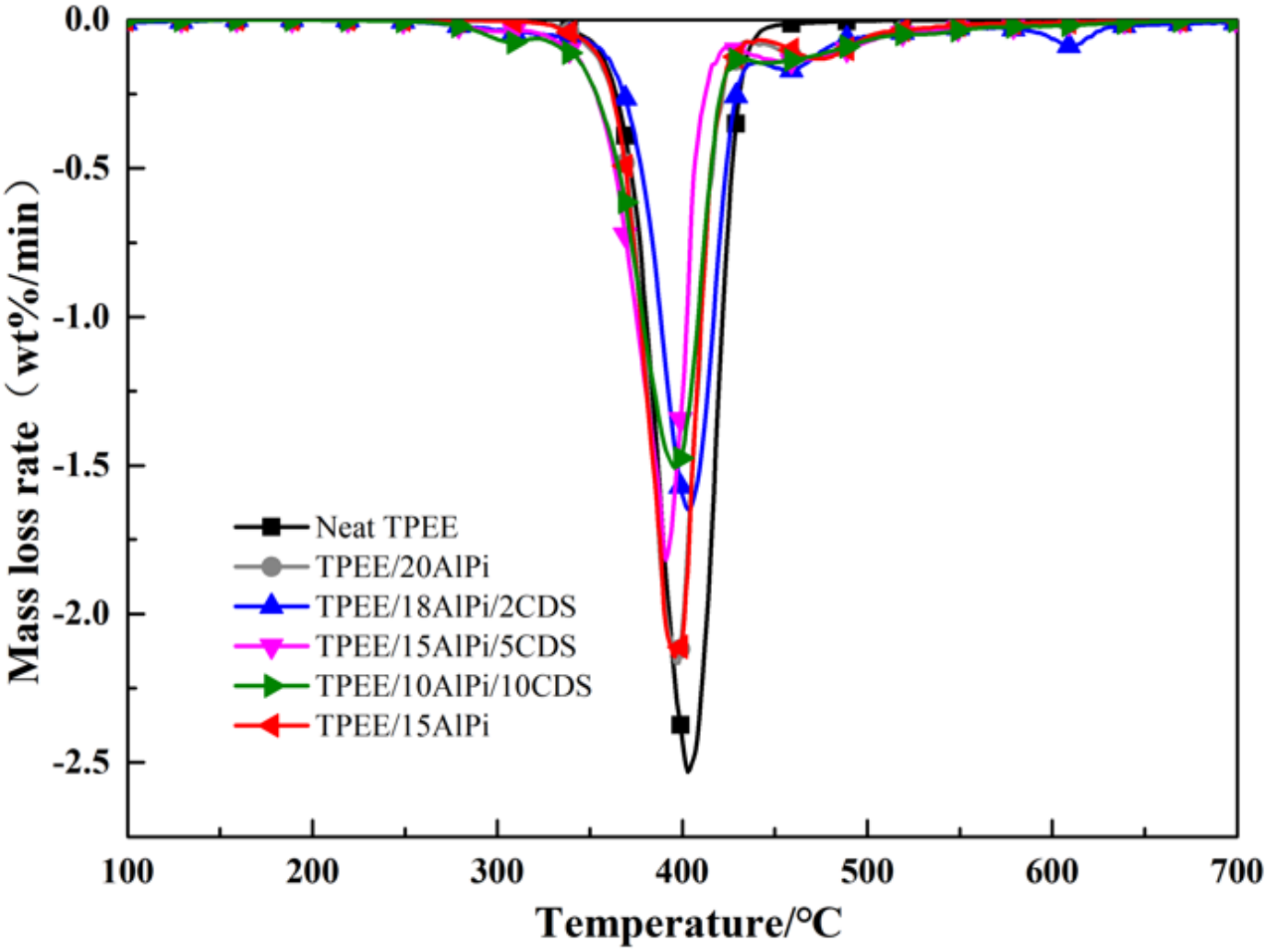

Figure 7

Mass loss rate curves of all the investigated samples (under nitrogen atmosphere, heating rate of 10°C/ min-1).

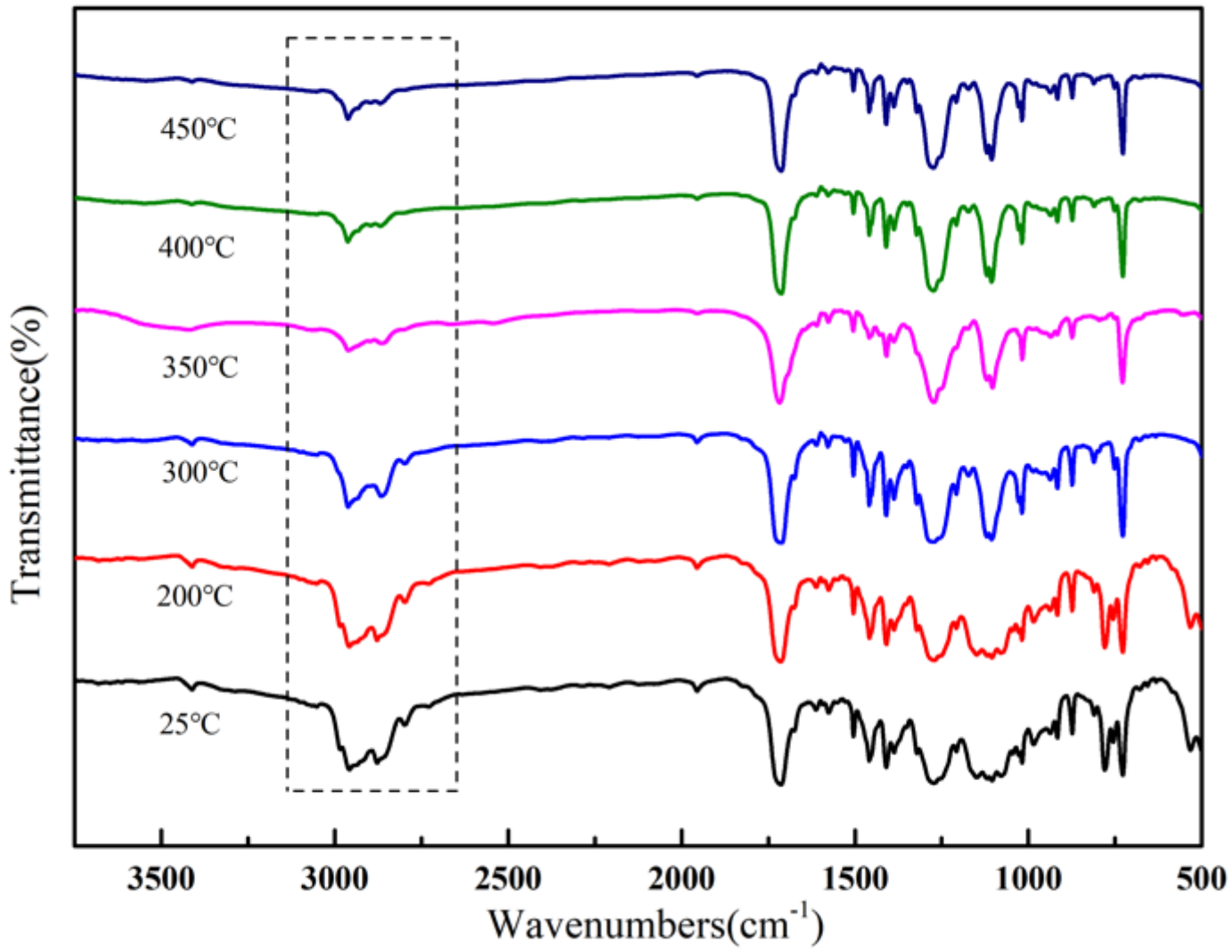

Figure 8

FTIR spectra of the solid phase in TPEE at different temperatures.

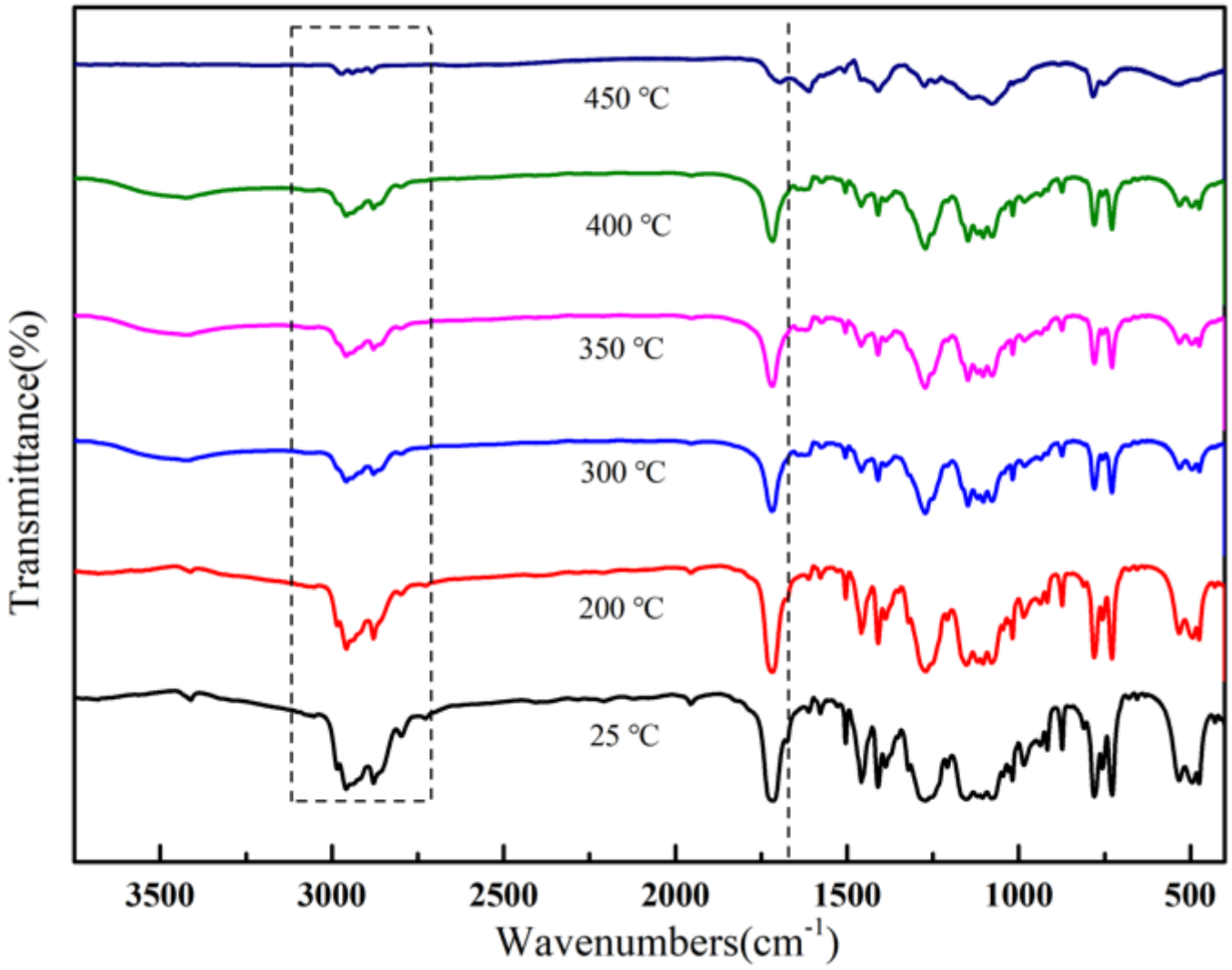

Figure 9

FTIR spectra of the solid phase in TPEE/15AlPi at different temperatures

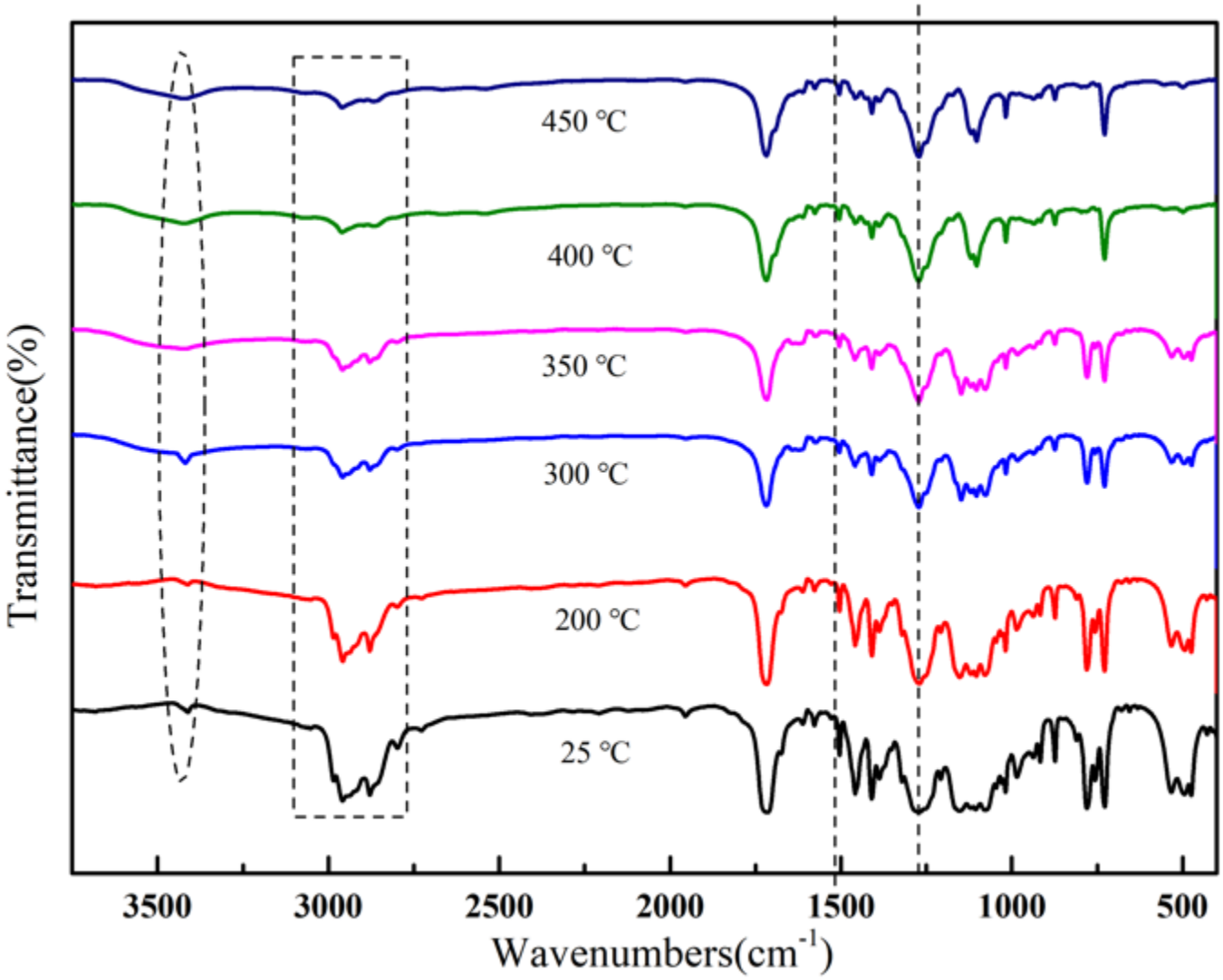

Figure 10

FTIR spectra of the solid phase in TPEE/AlPi/CDS at different temperatures

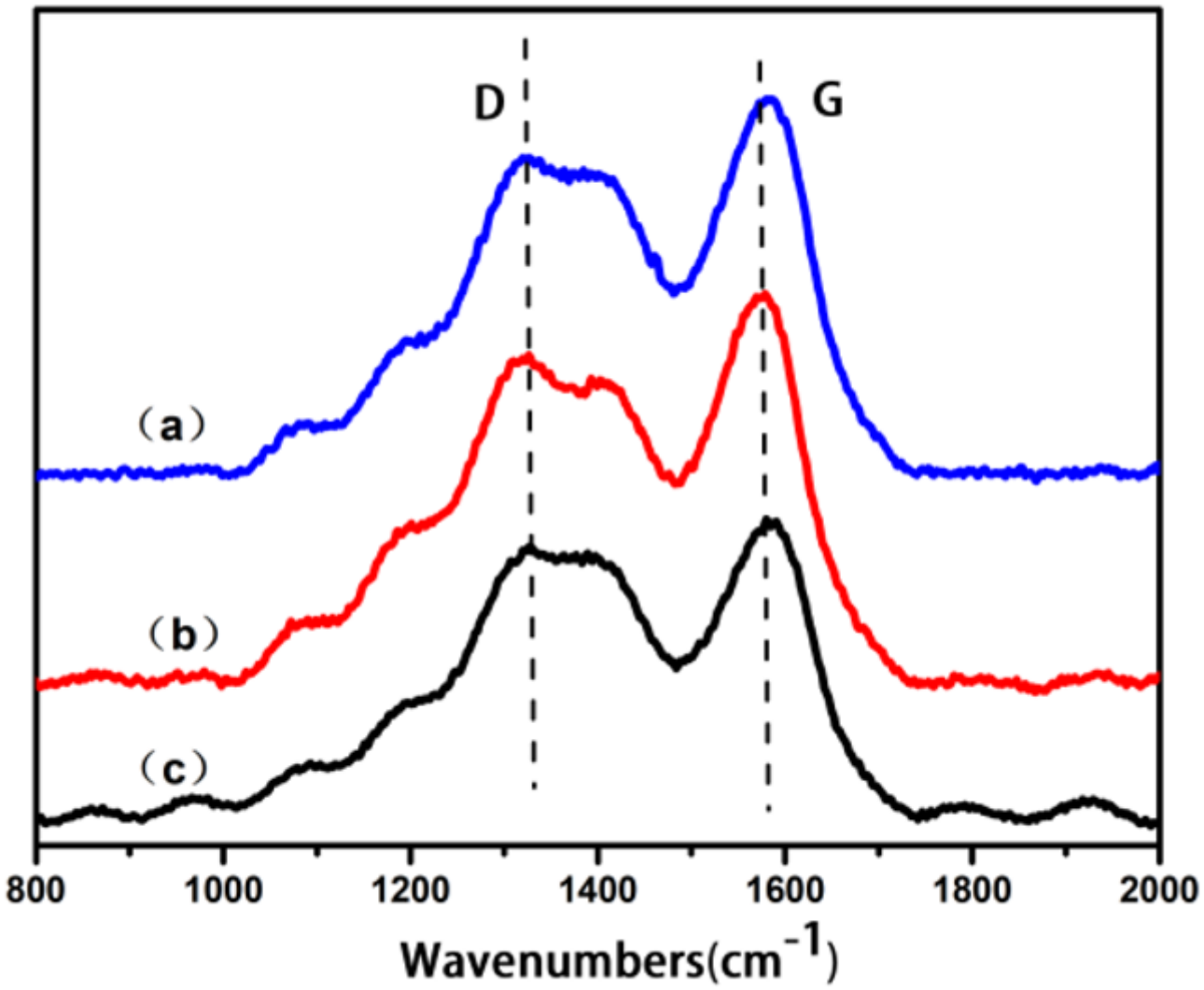

Figure 11

Raman curves of the char residues of (a)TPEE/20AlPi, TPEE/18AlPi/2CDS, and TPEE/15AlPi/5CDS after calcination at 700℃ for 15 min in a muffle furnace

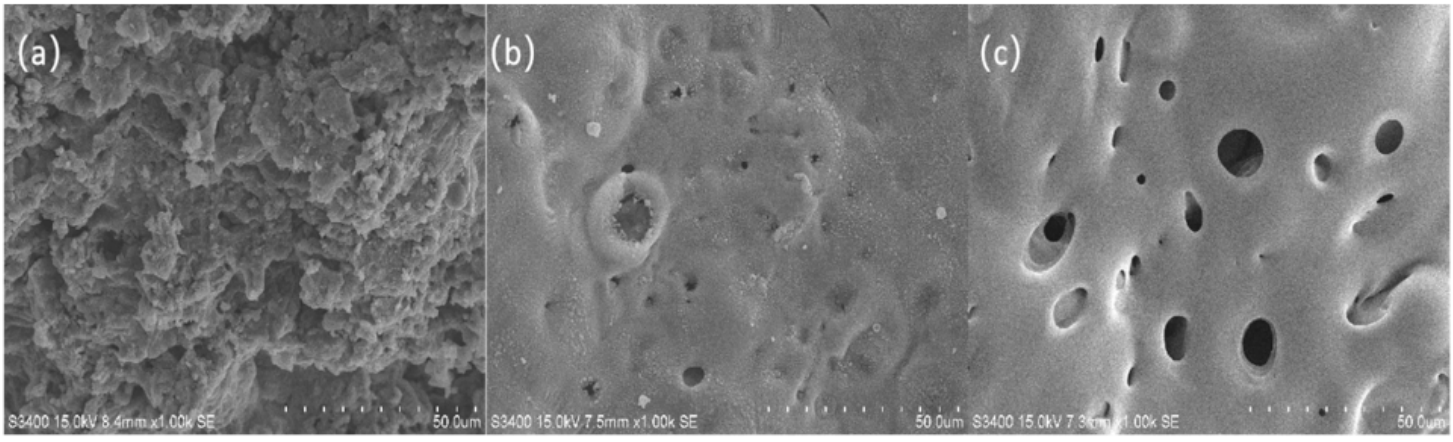

Figure 12

SEM images of the residue of (a)TPEE/20AlPi, TPEE/18AlPi/2CDS, and TPEE/15AlPi/5CDS at 50.0μm.

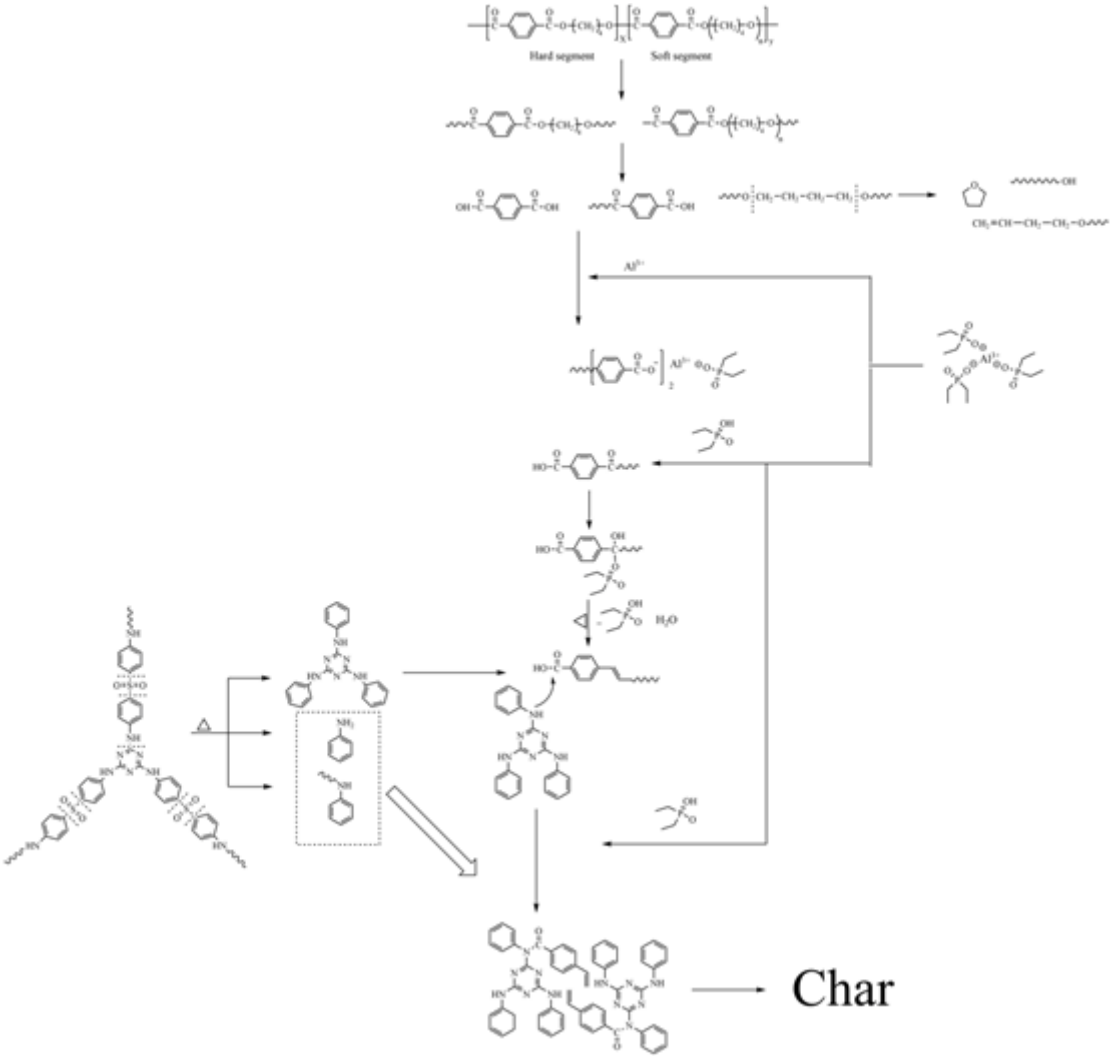

Figure 13

Main decomposition mode of TPEE/15AlPi/5CDS composite

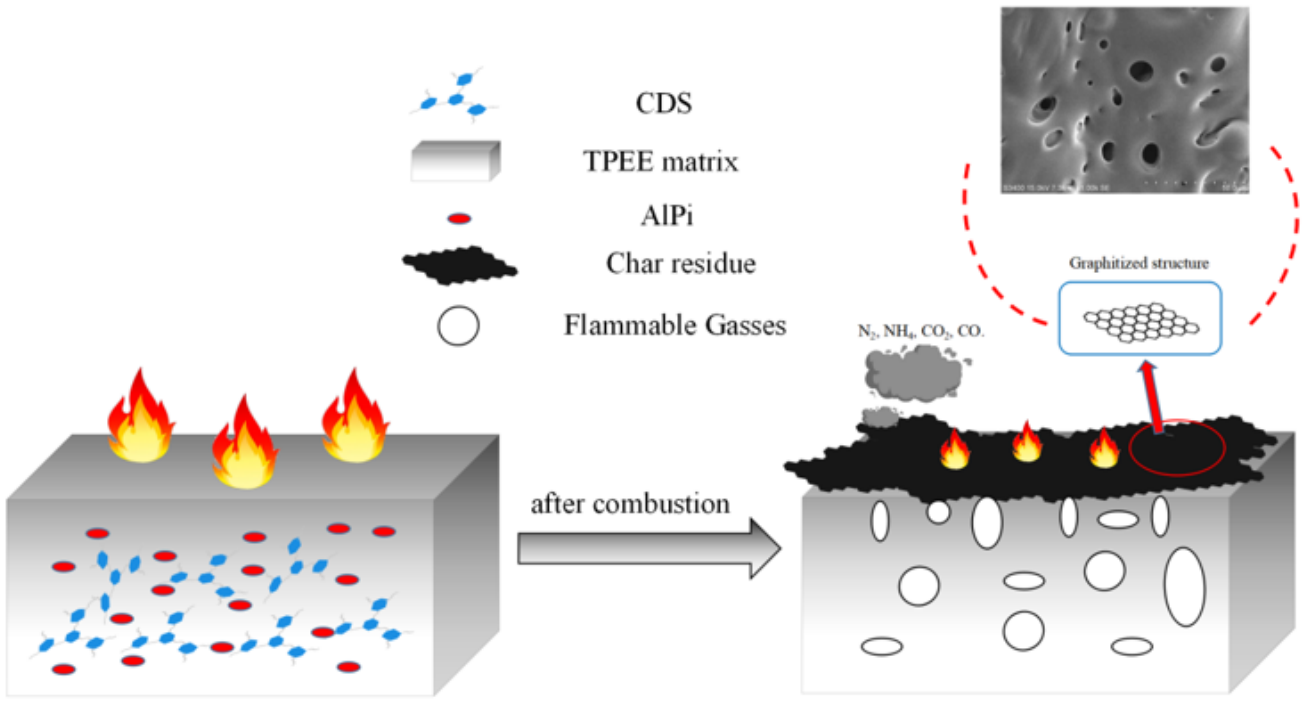

Figure 14

Schematic illustration of flame-retardant mechanism for CDS and AlPi in flaming of TPEE composites.